communications earth & environment

ARTICLE

https://doi.org/10.1038/s43247-023-00990-4 OPEN

Sea animal colonies enhance carbonyl sulfide emissions from coastal Antarctic tundra

Wanying Zhang [1], Renbin Zhu [1✉], Yi Jiao [2,3], Robert C. Rhew[4,5], Bowen Sun[1], Riikka Rinnan[2,3] & Zeming Zhou[1]

The Antarctic tundra, dominated by non-vascular photoautotrophs (NVP) like mosses and lichens, serves as an important habitat for sea animals. These animals contribute organic matter and oceanic sulfur to land, potentially influencing sulfur transformations. Here, we measured carbonyl sulfide (OCS) fluxes from the Antarctic tundra and linked them to soil biochemical properties. Results revealed that the NVP-dominated upland tundra acted as an OCS sink (-0.97 ± 0.57 pmol m^{-2} s^{-1}), driven by NVP and OCS-metabolizing enzymes from soil microbes (e.g., *Acidobacteria, Verrucomicrobia*, and *Chloroflexi*). In contrast, tundra within sea animal colonies exhibited OCS emissions up to 1.35 ± 0.38 pmol m^{-2} s^{-1}, resulting from the introduction of organosulfur compounds that stimulated concurrent OCS production. Furthermore, sea animal colonization likely influenced OCS-metabolizing microbial communities and further promoted OCS production. Overall, this study highlighted the role of sea animal activities in shaping the soil-atmospheric exchange of OCS through interacting with soil chemical properties and microbial compositions.

[1] Institute of Polar Environment and Anhui Provincial Key Laboratory of Polar Environment and Global Change, School of Earth and Space Sciences, University of Science and Technology of China, Hefei, Anhui 230026, China. [2] Terrestrial Ecology Section, Department of Biology, University of Copenhagen, Copenhagen Ø 2100, Denmark. [3] Center for Volatile Interactions (VOLT), Department of Biology, University of Copenhagen, Copenhagen Ø 2100, Denmark. [4] Department of Geography, University of California, Berkeley, CA 94720, USA. [5] Department of Environmental Science, Policy and Management, University of California, Berkeley, CA 94720, USA. ✉email: zhurb@ustc.edu.cn

Carbonyl sulfide (OCS) is the most long-lived and abundant sulfur-carrying gas in the atmosphere that can influence Earth's radiative balance by forming sulfate aerosols and affecting cloud condensation nuclei growth[1]. Major sources of atmospheric OCS include anthropogenic activities[2], oceans[3], biomass burning[4], volcanoes[5], and salt marshes[6], while sinks include OH oxidation in the troposphere[7], photolysis in the stratosphere[8], and plant uptake[9]. Soil plays a crucial role in the OCS exchange with the atmosphere as it functions as a bidirectional interface, usually depending on soil aeration and redox potential[10,11]. The atmospheric OCS mixing ratio varies both spatially and temporally, ranging between 360 and 560 parts per trillion (p.p.t), and is influenced by the relative contributions of sources and sinks[12].

Several studies have been conducted to quantify the exchange of OCS between ecosystems and the atmosphere[6,13–16]. These studies have revealed that vegetation is the primary sink for atmospheric OCS, with an estimated uptake of 500–1400 Gg equivalent-S annually[14–17]. However, the available observations have not covered all ecosystem types, which is essential for reliable bottom-up estimates of the global terrestrial OCS fluxes. For example, tundra ecosystems have thus far been overlooked. High-latitude tundra ecosystems are often covered by non-vascular photoautotrophs (NVP) such as mosses and lichens, which differ from vascular plants due to the absence of protective cuticles and responsive stomata. These differences may have an impact on the uptake of OCS[18].

Soil's role in OCS exchange with the atmosphere is not as well understood as that of aboveground vegetation. Plants usually exhibit a unidirectional uptake of OCS that is proportional to the gross assimilation of CO_2, which enables OCS flux measurements to serve as a useful proxy for estimating gross photosynthetic rates, such as gross primary productivity (GPP), at the ecosystem scale[19,20]. Soil OCS flux can complicate the OCS-derived estimates of stomatal conductance and GPP[21], and both OCS production and degradation in soil have been demonstrated[10,22]. OCS degradation can be catalyzed by carbonic anhydrase (CA), a ubiquitous enzyme that is present both within soil bacteria, fungi, and cyanobacteria[23–26] as well as extracellularly[27,28]. Enzymes like RuBisCO and nitrogenase also contribute to soil OCS degradation[29,30]. On the other hand, OCS can be produced in soil through biotic or abiotic processes. For example, saline microbial communities in salt marsh soils can mediate OCS production[6,31], and thiocyanate and CS_2 hydrolase mediated by soil microorganisms can also catalyze OCS production[32,33]. Heat- and solar radiation-induced soil organic matter decomposition can produce OCS, an abiotic process that is often regulated by the availability of organosulfur compounds in soil[22,34].

There are approximately 72,000 km^2 of ice-free tundra along the coast of Antarctica, which provides important habitats for sea animals such as penguins and seals[35,36]. These animals are persistently depositing organic matter and marine elements (including sulfur) into their terrestrial colonies, thereby altering the biogeochemical environment in coastal tundra ecosystems[37]. In zones not inhabited by sea animals, NVP is abundant and dominates the terrestrial surface. The soil-animal-NVP system in coastal Antarctica provides a unique, pristine environment for the study of sulfur transformation, especially the OCS exchange. Furthermore, the warming of the Antarctic is potentially promoting ice-free tundra expansion and seasonal permafrost thaw[38,39], which may further influence OCS exchange.

Overall, OCS exchange at the Antarctic tundra is a hitherto unexplored yet relevant component of the global sulfur cycle with potential climate feedback. We hypothesized that (1) soil OCS flux significantly contributes to the overall OCS flux in the Antarctic tundra; (2) sea animal colony tundra has a distinct OCS exchange pattern compared to that without sea animal influence; and (3) the presence of sea animals alters the community composition and activities of soil OCS-metabolizing microbes. In this study, we measured OCS fluxes with both in situ static chamber and laboratory-based incubation methods and examined the relationship between OCS fluxes and soil biological (bacterial and fungal community composition, OCS-metabolizing enzymatic activity) and physicochemical (nutrient, moisture, and pH) properties. With these analyses, we aimed to pinpoint the factors influencing OCS fluxes, explore OCS production and degradation mechanisms, and to elucidate the contribution of sea animals to OCS emissions from coastal Antarctic tundra.

Results

OCS flux from different Antarctic tundra. Upland tundra dominated by NVP showed a negative OCS flux, with an average rate of -0.97 ± 0.57 pmol m^{-2} s^{-1}, while both the seal and penguin colony tundra showed positive OCS fluxes, with average emission rates of 0.87 ± 0.69 pmol m^{-2} s^{-1} and 1.35 ± 0.38 pmol m^{-2} s^{-1}, respectively (Fig. 1a). There was a significant difference (LSD, $p < 0.05$) in OCS exchange rates between the upland tundra and penguin colony tundra, suggesting that the presence of sea animals or changes in NVP density has altered the OCS flux patterns in the tundra.

Soil OCS flux across different Antarctic tundra. Soils from five biogeographical zones of the Antarctic tundra were characterized by contrasting OCS flux directions and rates (Fig. 1b). Upland tundra soil (UTS) and tundra marsh soil (TMS) were found to be sinks of atmospheric OCS with average uptake rates of -0.93 ± 0.20 pmol 100 g $soil^{-1}$ min^{-1} and -0.45 ± 0.25 pmol 100 g $soil^{-1}$ min^{-1}, respectively. In contrast, soil samples collected from areas inhabited by sea animals such as the seal colony tundra (SCS), penguin colony tundra (PCS), and penguin-lingering tundra (PLS) were found to be sources of OCS. The highest OCS emission rates were observed in soil samples from the PCS, with an average rate of 1.97 ± 0.97 pmol 100 g $soil^{-1}$ min^{-1}. Both SCS and PLS soils exhibited OCS emissions, with average rates of 0.92 ± 0.58 pmol 100 g $soil^{-1}$ min^{-1} and 0.27 ± 0.14 pmol 100 g $soil^{-1}$ min^{-1}, respectively.

Both anoxic conditions and thermal sterilization treatments switched the UTS and TMS from OCS sinks to sources (Fig. 1b). For instance, UTS and TMS changed to emit OCS at a rate of 0.14 ± 0.04 pmol 100 g $soil^{-1}$ min^{-1} and 0.35 ± 0.11 pmol 100 g $soil^{-1}$ min^{-1}, respectively. After thermal sterilization treatments, the fluxes were at 0.20 ± 0.11 pmol 100 g $soil^{-1}$ min^{-1} and 1.59 ± 0.36 pmol 100 g $soil^{-1}$ min^{-1}, respectively. The soils from sea animal colonies (SCS and PCS) and the nearby region (PLS) remained as sources of OCS both under anoxic conditions and after thermal sterilization.

In the temperature range from −4 °C to 12 °C, UTS acted as OCS sinks, whereas sea animal colony soils (SCS and PCS) were consistent sources (Fig. 1c). OCS uptake in UTS showed a parabolic response to temperature ($R^2 = 0.956$, $p < 0.05$) with the highest rate observed between 0 and 8 °C at −1.10 to −0.93 pmol 100 g $soil^{-1}$ min^{-1}. The relationship between OCS emissions and temperature in SCS and PCS was better described by exponential regression, with Q_{10} values of 1.28 (95% confidential interval: 1.27–1.30) and 1.55 (95% CI: 1.36–1.78), respectively. The mean OCS fluxes were significantly lower in UTS than those in PCS and SCS (LSD, $p < 0.05$), indicating that the presence of sea animals altered the OCS flux pattern in tundra soils over a wide temperature range.

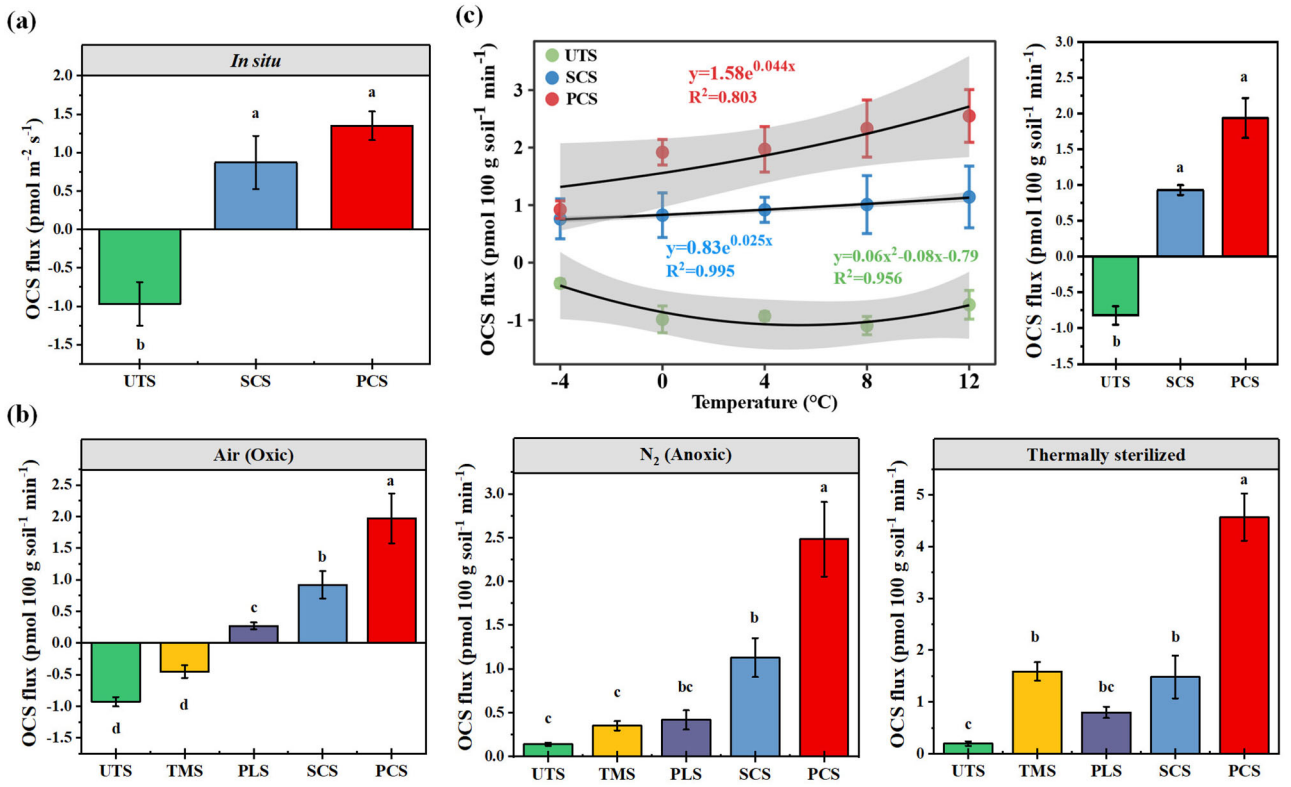

Fig. 1 Carbonyl sulfide (OCS) fluxes from the Antarctic tundra and soils. (**a**) OCS fluxes from in situ tundra static-chamber measurements ($n = 4$). (**b**) OCS fluxes from lab-based soil incubations at 4 °C under three different manipulated conditions: ambient conditions (oxic); pure N_2 conditions (anoxic); and autoclaved soil samples under ambient conditions (sterilized, oxic). (**c**) OCS fluxes from lab-based temperature-controlled soil incubations. Site name notes: UTS - upland tundra, SCS - seal colony tundra, PCS - penguin colony tundra, TMS - tundra marsh, PLS - penguin-lingering tundra. The letters (a, b, c, or d) indicate significant differences (LSD, $p < 0.05$) between the mean values of different sites. The shaded area in (**c**) represents the 95% confidence interval. Error bars represented the standard errors of the means.

Microbial composition and OCS-metabolizing enzymatic activity between sea animal colonies and animal-free region. The soils from penguin (PCS) and seal colonies (SCS) showed the highest bacterial richness, while there were no significant differences in bacterial diversity (as measured by Shannon and inverse Simpson indices) or evenness (Pielou's index) among the soils from different biogeographical zones (Supplementary Fig. 1). Principal coordinates analysis (PCoA) revealed that compositional differences in soil bacterial communities were separated between colonies (SCS, PCS) and animal-free zones (UTS, TMS, PLS) along the first axis, which explained 42% of the total variations (Fig. 2a). For fungal communities, PCoA showed that there was also a significant difference in fungal community structures between the soils from animal colony and animal-free zones (Fig. 2b). These results indicate that sea animal colonization has a significant impact on the microbial community structure in tundra soils.

At the phylum level, the dominant bacteria in tundra soils across different biogeographical zones were *Proteobacteria*, *Bacteroidetes*, *Acidobacteria*, and *Actinobacteria* (Fig. 2c). *Acidobacteria* or *Proteobacteria* were the major phyla in animal-free zones, while *Bacteroidetes* dominated in soil from animal colonies. In addition, soils from animal-free zones (UTS, TMS, PLS) had higher abundances of *Verrucomicrobia* and *Chloroflexi* compared to soils from animal colonies (SCS, PCS). For fungal communities, *Ascomycota*, *Basidiomycota*, and *Mortierellomycota* were dominant among the identified fungal phyla (Fig. 2d). Particularly, *Chytridiomycota* was the largest phylum in penguin colony soils. At the genus level, soils from animal-free zones were dominated by *DA101, Candidatus Solibacter*, and *Methylibium*, while soils from sea animal colonies featured a diversity of bacterial genera with even percentages, such as *Phormidium*, *Rhodoferax*, and *Dokdonella* (Supplementary Fig. 2; Supplementary Table 1). Canonical correspondence analysis (CCA) showed that the bacterial communities in soils from the animal colonies were influenced by total sulfur (TS), total nitrogen (TN), total phosphorus (TP), and total organic carbon (TOC), whereas the main soil physicochemical factors affecting fungal compositions included TS, pH, TP, etc (Supplementary Fig. 3; Supplementary Table 2).

Soils from animal colonies and animal-free regions also displayed different OCS-metabolizing enzymatic activities (Supplementary Fig. 4, Supplementary Note 1), with soils from the animal-free zone (UTS, TMS) featuring higher CA and RuBisCO activities. Sea animal colonization significantly decreased the activities of CA, RuBisCO, and nitrogenase in tundra soils (PCS, SCS, and the adjacent PLS) compared with UTS (LSD, $p < 0.05$).

Correlations between OCS flux and soil biochemical property. In situ, OCS fluxes from tundra were significantly correlated with soil moisture (Mc) and TS content ($r \geq 0.89$, $p < 0.05$) (Fig. 3a). Soil OCS fluxes from lab-based incubations were also significantly correlated with Mc, TS, TOC, TP, and TN ($r \geq 0.64$, $p < 0.05$) (Fig. 3b). It is noted that the soil contents of TS, TOC, TP, and TN, typically enhanced by sea animal activities[40,41], were intercorrelated with each other ($r \geq 0.69$, $p < 0.05$), suggesting that they were dominated by the same source, such as the deposition of sea animal excrement. A significant negative correlation was observed between soil OCS fluxes and CA enzyme activity ($r = -0.87$, $p < 0.001$), while no such correlation was found for the other

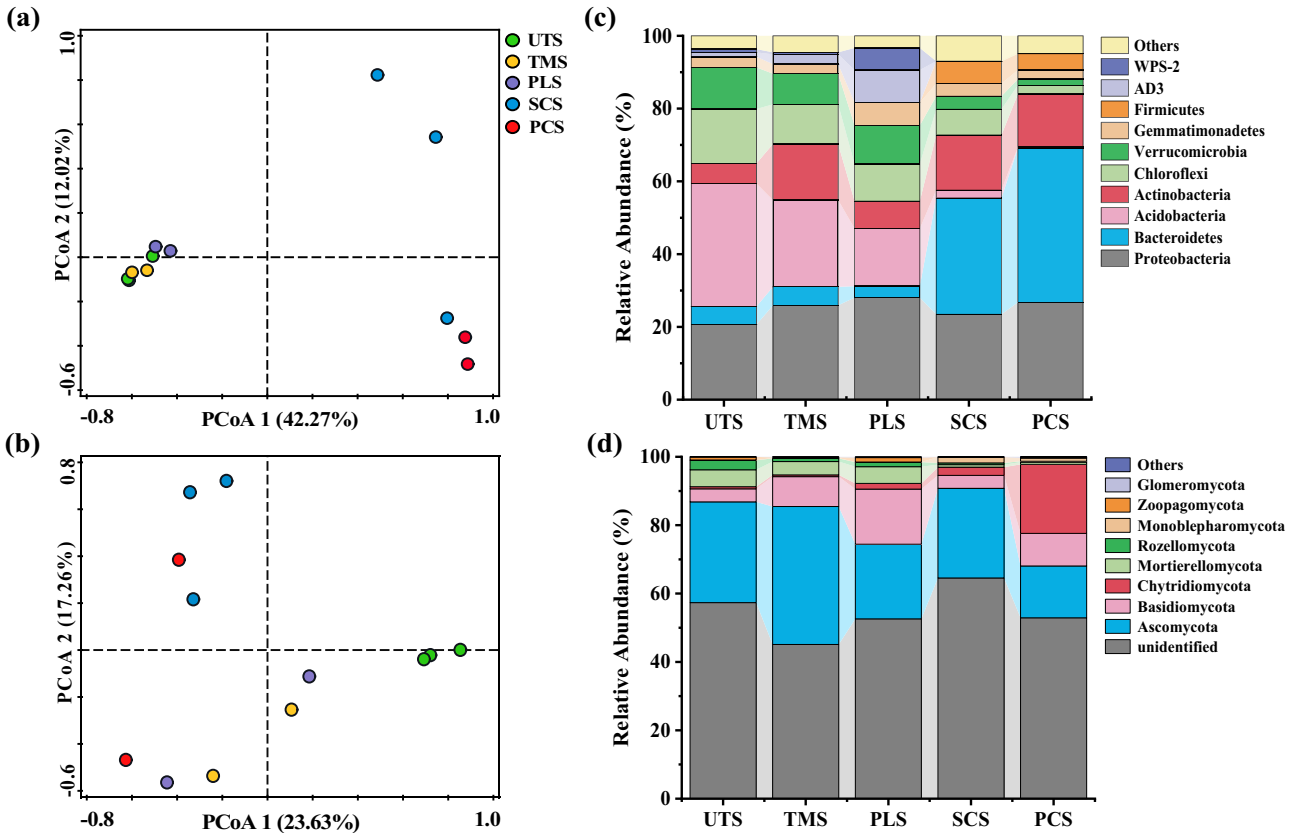

Fig. 2 Bacterial and fungal community compositions in the Antarctic tundra soils. Principle coordinates analysis (PCoA) plots for (**a**) bacterial and (**b**) fungal communities in all soil samples based on Bray–Curtis dissimilarity. Relative abundances of (**c**) bacterial and (**d**) fungal phyla in the soil samples across different tundra biogeographical zones. Site name notes: UTS upland tundra, TMS tundra marsh, SCS seal colony tundra, PCS penguin colony tundra, PLS penguin-lingering tundra.

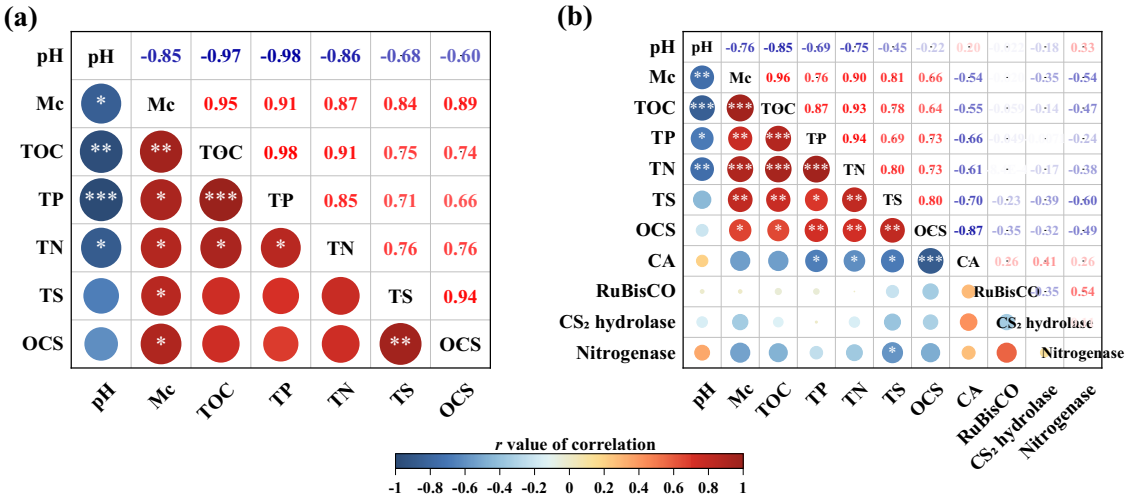

Fig. 3 Pearson correlations between OCS flux and different physiochemical parameters of the soils. (**a**) in situ static chamber measurements and (**b**) laboratory-based incubations. *$p < 0.05$, **$p < 0.01$, and ***$p < 0.001$. The numbers in the cells are r values with color scales between −1 and 1. The size of the circles represented the absolute value of correlation. Mc soil moisture, TOC total organic carbon, TP total phosphorus, TN total nitrogen, and, TS total sulfur.

types of OCS metabolism enzymes: RuBisCO, nitrogenase, and CS_2 hydrolase.

Correlations between OCS flux and OCS-metabolizing enzymatic activity and soil microbial community composition. Correlation analysis showed that the abundance of several dominant microbial phyla in the animal-free zone, including *Chloroflexi*, *Acidobacteria*, *Verrucomicrobia*, *Mortierellomycota* and *Planctomycetes*, had a positive correlation with soil CA activity and a negative correlation with OCS fluxes (Fig. 4a, b and Supplementary Fig. 5). Conversely, the largest bacterial phylum in animal colonies, *Bacteroidetes*, had a negative correlation with soil

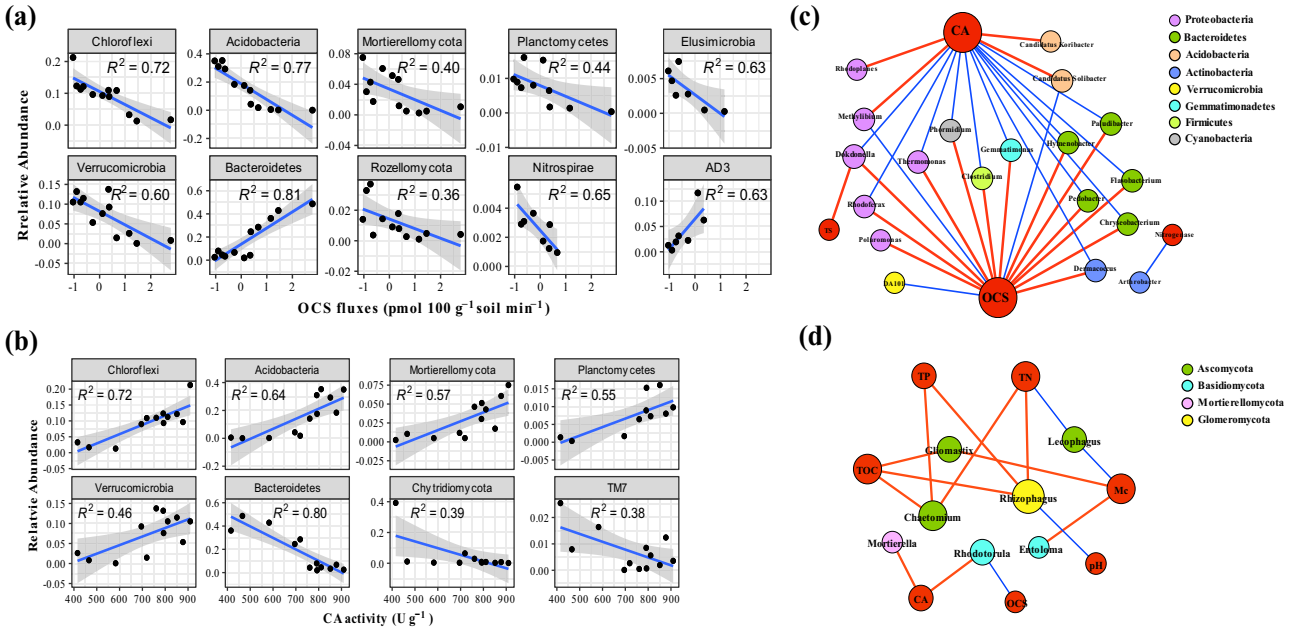

Fig. 4 Correlation analysis between soil microbial phylum abundances, OCS fluxes, and CA enzyme activities. Correlations between observed soil microbial phylum abundances and (**a**) soil OCS fluxes or (**b**) soil carbon anhydrase (CA) enzymatic activities, and network analysis based on correlations between (**c**) bacterial genera or (**d**) fungal genera and OCS fluxes, soil CA activities and other properties. Only significant correlations ($p < 0.05$) are presented. The shaded areas in (**a**) and (**b**) represent the 95% confidence intervals ($p < 0.05$), and the red and blue lines in (**c**) and (**d**) indicate positive and negative correlations, respectively. For microbial genera, the circles sharing the same color belong to the same phylum.

CA activity but a positive correlation with OCS fluxes. A positive relationship was also observed between nitrogenase and the abundance of bacterial *Acidobacteria* and fungal *Rozellomycota*, which was of higher abundance in animal-free soils featuring higher OCS uptake fluxes.

At the genus level, bacteria *Candidatus Solibacter*, *Methylibium*, *DA101*, and fungal *Rhodotorula*, which were the dominant genera in the soils from the animal-free zone, were positively correlated with soil CA enzymatic activities and negatively correlated with soil OCS fluxes (Figs. 4c, d). A positive relationship was also observed between nitrogenase and the abundance of bacterial *Acidobacteria* and fungal *Rozellomycota*, which was of higher abundance in animal-free soils featuring higher OCS uptake fluxes. Additionally, several minority bacterial genera in the soils showed a negative relationship with CA enzymes and positive OCS fluxes, such as *Paludibacter*, *Thermomonas*, and *Dermacoccas*.

Discussion

Simultaneous OCS degradation and production in Antarctic tundra soils. This study revealed that OCS fluxes varied across the five biogeographical zones of the Antarctic tundra. Notably, soils from animal-free regions were observed to act as OCS sinks, a pattern consistent with soils from most other global ecosystems[34,42–44]. On the other hand, soils from animal colonies were OCS sources, similar to anoxic soils of wetlands and some oxic soils[6,34,45].

The degradation of atmospheric OCS in soil is believed to be catalyzed by carbonic anhydrase (CA), an enzyme that can be produced by soil fungi, bacteria, and cyanobacteria[27,28]. Soil fungi *Ascomycota* and bacteria *Actinobacteria* (the phylum to which *Mycobacteria* belongs) were known to be able to release CA enzymes[23,24,26,27] and they were among the dominant fungal and bacterial communities in the Antarctic tundra soil (Fig. 2). More specifically, it was found that CA enzymatic activities were negatively correlated with soil OCS fluxes (Fig. 3), further supporting that the CA enzyme may be responsible for the degradation of atmospheric OCS in soil[26,31,46].

In addition to these previously reported OCS-metabolizing microbes, our findings showed that the abundance of *Acidobacteria*, *Verrucomicrobia*, *Chloroflexi*, and *Mortierellomycota*, as well as the genera *Candidatus Solibacter*, *Methyllibium*, *Rhodoplanes*, and *Rhodotorula* were positively correlated with CA activity and negatively correlated with OCS flux (Fig. 4), which indicated that these dominant microbial phyla/genera may also be able to secrete CA and play a role in OCS degradation. Furthermore, the presence of nitrogenase enzymes was positively related to bacterial *Acidobacteria* and fungal *Rozellomycota*, particularly in soils outside of animal colonies, suggesting a potential OCS-metabolizing role for these microbes as well.

On the other hand, our study did not quantitatively assess the abundance of OCS-metabolizing microbial communities. Future research using techniques like real-time qPCR may help reveal the specific bacterial and fungal species involved in OCS metabolism, thereby enhancing our understanding of the abundance and distribution of these microbial communities and their impact on OCS dynamics in the ecosystem.

The efficacy of CA in catalyzing OCS degradation would be irreversibly reduced if temperatures exceed 55–80 °C[28,47,48]. In this study, thermal sterilization treatment of soils, which could effectively deactivate the CA during the treatment, switched UTS and TMS from OCS sinks to sources (Fig. 1b). This further supports the hypothesis that CA catalysis was important in OCS degradation. On the other hand, net OCS emissions after the thermal treatment of soils suggested the likely existence of simultaneous abiotic production of OCS in tundra soils, which could be previously obscured by the biogenic sink of the active CA enzyme.

Sea animal activities promote soil OCS production. In contrast to the areas free of sea animal influence, soils from sea animal colonies and the adjacent tundra were observed as OCS sources.

Table 1 Physiochemical properties in tundra soils in coastal Antarctica.

Tundra sites	pH	TOC (%)	TN (mg g^{-1})	TP (mg g^{-1})	TS (mg g^{-1})	Mc (%)
UTS	6.7 ± 0.4^{b}	2.9 ± 0.6^{a}	3.4 ± 1.4^{a}	2.1 ± 0.2^{a}	1.0 ± 0.4^{a}	13.5 ± 2.9^{a}
SCS	6.9 ± 0.4^{b}	4.6 ± 0.5^{b}	6.4 ± 2.7^{a,b}	2.7 ± 0.3^{a}	2.9 ± 0.4^{b}	29.3 ± 7.2^{b}
TMS	5.4 ± 0.0^{a}	8.6 ± 1.9^{c}	10.4 ± 0.5^{b,c}	4.4 ± 1.4^{a}	2.1 ± 0.3^{a,b}	47.6 ± 8.7^{c}
PLS	4.9 ± 0.1^{a}	9.4 ± 1.2^{c}	13.0 ± 2.4^{c,d}	12.9 ± 2.7^{b}	2.9 ± 0.4^{b}	41.4 ± 2.6^{c}
PCS	5.0 ± 0.2^{a}	12.6 ± 1.4^{d}	17.8 ± 6.3^{d}	19.6 ± 7.7^{b}	4.3 ± 1.0^{c}	59.4 ± 4.6^{d}

Values sharing the same lower-case letter (a, b, c, or d) do not differ significantly (LSD, $p < 0.05$).

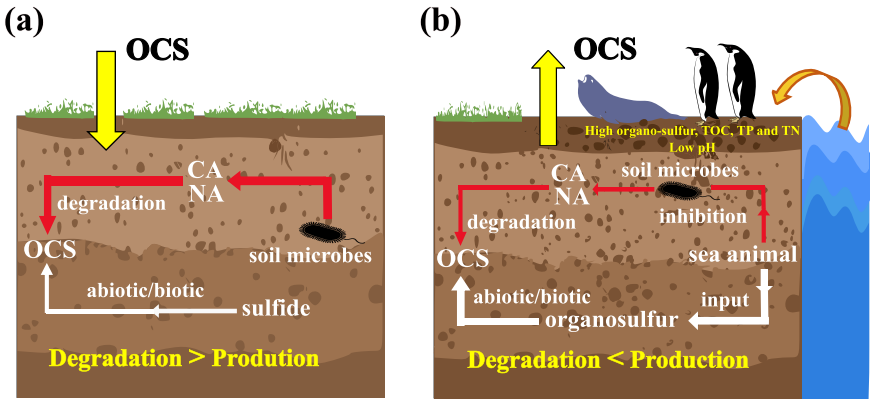

Fig. 5 Conceptual drawing for the potential mechanisms of OCS production and degradation in the Antarctic tundra. (**a**) without sea animal influence, and (**b**) with or adjacent to sea animal colonies in coastal Antarctica. CA and NA indicate carbonic anhydrase and nitrogenase enzymes, which are excreted by tundra soil microbes. The white and red lines indicate OCS production and degradation processes, respectively. Line thickness indicates the relative rate of the process.

The presence of penguin and seal activities in these areas may have played a role in the production of OCS in the tundra soils.

Firstly, increased levels of TS were observed in soils of sea animal colonies, as a result of the terrestrial input of oceanic sulfur from penguin guano, which served as substrates for OCS production (Table 1 and Supplementary Table 3). The sediments in penguin colonies had a high concentration of sulfur, dominated by organosulfur (66.7%), sulfate (23.4%), and reduced inorganic sulfur (9.9%), such as acid volatile sulfur and pyrite sulfur[37,49]. These substances may be converted into volatile sulfur trace gases, including OCS, as observed in the study, and some other volatile sulfur compounds such as dimethyl trisulfide, dimethyl tetrasulfide, and dimethyl pentasulfide[50]. Similarly, reduced volatile sulfur compounds such as OCS and dimethyl sulfide (DMS) are produced during the degradation of fresh excrement in the poultry industry[51,52]. In addition, soils in the penguin colony and its adjacent tundra also showed high N and P levels and lower pH due to the input of guano. Several empirical studies have confirmed that soil OCS production is usually enhanced in low-pH and high-N environments[25,26,53]. Therefore, the high-S, high-N, and low pH characteristics of the sea animal colony soils may support enhanced OCS production through undetermined mechanisms.

Secondly, sulfate reduction metabolism in anoxic environments is usually responsible for soil OCS production, such as in salt marshes[6] and rice paddies[42,54,55]. The soil in sea animal colonies is often anoxic due to the low-elevation coastal location subject to frequent inundation by seasonal snowmelt, which can lead to saturated soils that limit oxygen diffusion into soil pore space. The results from our lab incubations under an anoxic environment further implied that the production of OCS in Antarctic sea animal colonies was associated with the anoxic soil environment induced by sea animal activities.

Thirdly, penguin and seal inputs to their colony tundra may have suppressed the abundance of OCS-metabolizing microbes, such as *Candidatus Solibacter*, *Methyllibium*, *Rhodoplanes*, and *Rhodotorula*, and/or promoting the growth of OCS-emitting microbes, such as *Bacteriodetes*, thereby enhancing the OCS production from soils.

The production of OCS through the exposure of soil organic matter to high light or temperatures has been reported in previous studies[22,34,45]. However, considering the polar location of our study, it is unlikely that this mechanism can fully explain the in situ production of OCS observed in this study. Nonetheless, it cannot completely dismiss the possibility that the observed OCS emissions after thermal treatment were derived from accumulated OCS in soil pores during the thermal degradation of organosulfur. Future investigations could employ soil sterilization techniques that minimize disturbance to soil organic matter[56], such as gamma-irradiation and chemical amendment. These approaches may provide a clearer understanding of whether thermal degradation of soil organosulfur contributes to OCS production.

In light of our findings, it can be inferred that sea animal activities play a significant role in the enhanced production of OCS from soils. This effect is primarily attributed to two key factors: the promotion of OCS production through the introduction of animal-derived organosulfur compounds and the likely influence on the production and degradation of OCS via alterations in the soil microbial community (Fig. 5).

Potential OCS uptake by NVP. In situ measurements showed that upland tundra acted as a sink for atmospheric OCS. In addition to the microbial sink in the soils, surface NVP may have also contributed to the uptake of OCS. Some NVP, such as the

mosses *Alectoria sormentosa* and *Scleropodium purum*, the liverwort *Marchantia polymorpha*, and the lichen *Ramalina menzlesii*, could uptake atmospheric OCS[18,57–61]. Similarly, the upland tundra was covered by mosses (*Drepanocladus uncinatus* and *Bryum pseudotriquetrum*), and some sporadic lichens (*Usnea* sp.), which may also be capable of consuming OCS at ambient atmospheric concentrations.

The uptake of OCS and CO_2 by plants usually shares the same enzymes[62]. Photosynthetic activities of NVP species are usually only 10% or less of those observed from higher vascular plants[63]. Accordingly, a much lower uptake rate of OCS was observed in comparison to other vascular plant ecosystems (Supplementary Table 4), which was likely attributed to the lower CA enzyme activity in these NVP[64]. For example, the observed OCS uptake rates from normal tundra were much smaller than other reported plant sinks, such as temperate and subtropical grassland[43,65], temperate and boreal forest[66–69], and agricultural fields[53].

The tundra within sea animal colonies, however, were found to be sources of OCS. The aboveground biogenic OCS sinks, such as surface NVP, were reduced due to daily trampling and over-manuring caused by the deposition of excessive animal guano[70]. Consequently, the aboveground biogenic OCS sinks were outweighed by the soil emissions, which turned them into overall sources of OCS.

The presence of bidirectional soil OCS fluxes can complicate the estimation of ecosystem GPP based on OCS fluxes, particularly when the soil flux is comparable to the plant flux[67,71,72]. In Antarctic tundra ecosystems, the limited OCS uptake capability of NVP may further contribute to this interference. Additionally, the current global soil OCS flux model lacks comprehensive measurements from NVP ecosystems in high latitudes[21]. Therefore, it is essential to conduct more field-based or laboratory-based measurements of OCS fluxes in the Antarctic tundra, especially in NVP-dominated areas, in order to improve the accuracy of calculating OCS-derived GPP.

Temperature effect on OCS emissions. The Antarctic region, especially the peninsular area, is experiencing unprecedented and faster warming compared to the rest of the globe[38,39]. The OCS emission rates from soils in seal and penguin colony tundra increased with soil temperatures from −4 °C to 12 °C (Fig. 1c), indicating that OCS emissions from these sea animal colonies will still be enhanced in the projected warming future in Antarctica. Additionally, the rapid warming of the continent is leading to a larger area of ice-free tundra and affecting the size of penguin and seal populations and colonies[38], which suggests that the contribution of penguin and seal colony tundra ecosystems to atmospheric OCS may be enlarged in response to future climate change.

To conclude, soils in the Antarctic tundra acted as important bidirectional interfaces of atmospheric OCS. The presence of organic matter and oceanic sulfur from sea animals impacted the soil microbial communities and nutrient contents, resulting in changes in sulfur transformations: soils without animal influence can take up OCS, primarily due to carbonic anhydrase produced by soil microbes, whereas soils near animal colonies were OCS sources, mainly originating from fermentation of organosulfur from the sea animals. This research underscores the impact of sea animal activities on soil function as an interface of atmospheric OCS, via interactions with soil chemical properties and microbial compositions.

Methods

Site description. The study region (Supplementary Fig. 6) is located in the Antarctic Peninsula and is characterized by a sub-Antarctic oceanic climate. Meteorological records from the Antarctic Great Wall Research Station showed an average annual temperature of approximately −2.5 °C, ranging from −26.6 to 11.7 °C, and an average annual precipitation of 630 mm. The fieldwork was conducted in two areas of the region: Fildes Peninsula (61°51′S-62°15′S, 57°30′W-59°00′W) and Ardley Island (62°13′S, 58°56′W).

The Fildes Peninsula is the largest ice-free area on King George Island. The middle of the peninsula is bedrock-exposed hills; a well-developed tundra ecosystem is distributed along the coastline, with mosses (*Drepanocladus uncinatus* and *Bryum pseudotriquetrum*), and lichens (*Usnea* sp.) as the dominant vegetation. The western coast of the peninsula is inhabited by seals. In this area, 5 study sites were selected for both seal colony tundra (S1-5, Supplementary Fig. 6) and upland tundra without sea animal influence (U1-5, Supplementary Fig. 6).

The study area at Ardley Island features a penguin habitat with a population of over 10,000 individuals on its eastern side[35]. Penguins can occasionally be found in the middle of the island. The western side of the island is a lowland tundra marsh characterized by cushions of mosses, lichens, and algae. In accordance with the east-middle-west biogeographical gradient, 4 study sites were selected in the penguin colony tundra (P1-4), 2 in the penguin-lingering tundra (PL1-2), and 2 in the tundra marsh (M1-2).

The different biogeographical zones of the study areas were characteristic of different soil properties such as moisture, total organic carbon (TOC), total nitrogen (TN), total phosphorus (TP)[70,73,74]. In general, soils in animal colonies had higher nutrient levels than those in animal-free tundra. Particularly, the total sulfur (TS) content was higher in the animal colony soils than in the animal-free tundra soils, with the penguin colony having the highest TS content ($4.3 \pm 1.0\ mg\ g^{-1}$), about four times higher than that in the upland tundra (Supplementary Note 2, Table 1, and Supplementary Table 3).

OCS flux measurements

In situ measurements. In situ measurements of trace gas fluxes were taken in January 2020 (10:00–12:00 UTC-03) at seal colony tundra (S1-2), penguin colony tundra (P1-2), and upland tundra (U1-2). In this field campaign, several trace gases were measured, including OCS and some halogenated compounds[70,75]. The static chamber deployed consisted of a base (50 cm × 50 cm × 5 cm) and a lid (50 cm × 50 cm × 25 cm), forming a closed headspace with water sealing between the base and lid. The chamber bases were installed at each site 2 days ahead of the first sampling to stabilize and reduce any potential perturbations. Air samples were taken from the chamber headspace into 1-liter pre-evacuated flasks (Entech, California) at 1, 16, and 31 minutes after chamber closure via a stainless-steel tube extended to the center of the headspace. Two independent replicate static chamber measurements were conducted at each site.

The analysis of OCS in the air samples was performed using a gas chromatograph-mass spectrometer (GC/MS, 7890B/5973 N, Agilent Technologies, California, United States) equipped with a cryotrapping pre-concentrator (7100 A, Entech, California, United States). 0.3 L of each air sample was first cryofocused at −40 °C. Subsequently, samples in the first trap were heated to 10 °C, and transported to a secondary trap at −40 °C to remove H_2O and CO_2. Samples were further heated to 180 °C to transfer to a third trap and trapped at −160 °C, which was heated up to 80 °C rapidly at the last to inject samples into an HP−1 capillary column (60 m × 0.32 mm × 1.0 μm, Agilent Technologies, California, United States) of GC/MS. GC temperature was programmed in the following procedure: it was initially held at 10 °C

for 3 min, heated to 120 °C at 5 °C min^{-1}, then heated at 10 °C min^{-1} up to 250 °C and held for 7 min. The samples were calibrated against a commercial standard mixture containing 23 volatile organic compounds, including OCS at 157 p.p.t. (mixed and calibrated at Guangzhou Institute of Geochemistry, Chinese Academy of Sciences) using an internal standard method[75].

Soil sample collection and laboratory incubation. Surface soil samples (0–10 cm depth) were collected from all study sites. Soil samples were preserved at −20 °C prior to laboratory analysis and incubation. In the laboratory, soil samples were thawed overnight at room temperature, and then their physical and chemical properties were measured, including soil pH, gravimetric moisture content (Mc), TOC, TN, TP, and TS contents (Supplementary Table 3).

Soil samples were incubated under controlled conditions for OCS fluxes. For each soil sample from the selected sites (S3-5, U3-5; M1-2, PL1-2, P3−4), 25 g (fresh weight) were enclosed in glass jars (1.9 L) and incubated over 12 h at 4 °C (in situ average summer temperature) using a water/ethylene glycol bath (VWR Model 1180 S, Pennsylvania, United States). The glass jars were connected to a pre-evacuated stainless-steel coiled tube (25 mL), which was part of the inlet tube of the cryo-trapping system (HayeSep® D 100/120 mesh porous polymer adsorbent, sealed with glass wool) of a gas chromatograph/mass spectrometer (GC/MS; Agilent 6890 N/5973, Agilent Technologies, California, United States)[76]. The headspace air in the jars was drawn, cryotrapped (dry ice/ethanol bath, ~ −85 °C), and injected into the GC/MS for OCS analysis 1, 31, and 61 min after sealing the jars, based upon which the flux was calculated.

The incubations were repeated under three different treatments using independent soil samples: (1) ambient air condition, (2) anoxic condition, and (3) post-thermal sterilization. The anoxic condition was accomplished by flushing and filling the jar headspace with ultra-pure nitrogen gas (≥99.999%, Praxair, Connecticut, United States) for a week. Thermal sterilization was conducted by autoclaving the soil samples at 150 °C for 2 h. After the thermal sterilization, the soil samples were allowed to vent to the ambient air overnight. Subsequently, they were flushed with ambient air for several minutes before the incubations began. This procedure aimed to minimize the presence of accumulated OCS gas in the soil pores to the best extent possible. Additionally, to understand the relationship between OCS fluxes and temperature, independent soil samples (U3-5; S3-5; P3-4) were also incubated at 4 °C intervals between −4 °C and 12 °C under ambient air condition in the same method above.

The calibration of the GC/MS in these soil incubations was performed using a natural air standard collected and calibrated at the Scripps Institution of Oceanography (SIO-98 calibration scale). The same standard was run before and after each batch of incubations on the same day to correct for the daily drift of the mass spectrometer signal.

Flux calculation. The OCS fluxes (F) were calculated by fitting the OCS molar fraction to the time of enclosure using linear least squares, normalizing to the enclosed surface area (for in situ measurements) or soil sample mass (for lab soil incubations), and multiplying by the number of moles of air in the measurement chamber or jar.

$$F = \frac{1}{A}\frac{dc}{dt}N_a \quad (1)$$

where A represents the surface area or the soil mass; dc/dt is the slope of the linear least squares fit, and N_a is the number of moles of air in the chamber or jar. To allow comparison with the review literature[17], the OCS fluxes from chamber measurements are reported in pmol m^{-2} s^{-1}, and the fluxes from soil incubations are reported in pmol 100 g $soil^{-1}$ min^{-1}. Positive fluxes represent OCS emissions to the atmosphere, whereas negative fluxes represent OCS deposition or degradation.

For measurements with linear correlation coefficients <0.8, we assume that the OCS change in the headspace follows an exponential relationship with time[77]:

$$[c]_t = [MAX] - \left([MAX] - [c]_0\right)e^{-kt} \quad (2)$$

where [MAX] represents the maximum OCS concentration reached when the gas concentration within the enclosure headspace equals that of the soil atmosphere, $[c]_0$ is the initial OCS concentration in the headspace, and k is a rate constant. [MAX] and k were solved iteratively[6], and then OCS fluxes at $t = 0$ were calculated by the following equation:

$$F = k\left([MAX] - [c]_0\right) \quad (3)$$

Blank measurements were conducted to account for the detection limit and potential errors associated with chamber materials (±0.12 pmol m^{-2} s^{-1}). Only fluxes above the detection limit were reported in the study.

Determination of soil enzymatic activities and microbial community compositions. We investigated the impact of soil enzymes and microbial communities on OCS fluxes in selected soil samples (S3-5, U3-5; M1-2, PL1-2, P3-4). The activity of OCS-metabolizing enzymes, such as carbonic anhydrase (CA), RuBisCO, nitrogenase, and CS_2 hydrolase, was determined using an enzyme-linked immunosorbent assay (ELISA) method[78] and expressed in units U g^{-1} soil. First, we used a purified CA antibody to coat the microplate to make a solid-phase antibody. Afterward, CA was added through the micropores of the microplate, and then bound with horseradish peroxidase (HRP)-labelled antibody to form the "antibody-antigen-HRP-labeled antibody" complex. This complex was then mixed with TMB (3,3′,5,5′-tetramethylbenzidine), a chromagen substrate, which produces a yellow color reaction under the catalysis of HRP. The shade of yellow is positively correlated with carbonic anhydrase (CA) in the samples. The absorbance (optical depth) of the mixture was measured with a microplate reader (λ = 450 nm). Calibration curves were constructed with standard enzymatic solutions. The same analytical procedure was used for RuBisCO, nitrogenase, and CS_2 hydrolase.

The microbial community composition was analyzed in the following sequence: (1) microbial genomic DNA extraction from soil samples, (2) amplification of DNA using universal primer sets and purification, and (3) downstream sequencing of DNA using NCBI GenBank[79]. In detail, microbial genomic DNA was extracted from 0.25 g soil using the DNeasy Powersoil Kit (MoBio, USA). The concentration of extracted DNA was measured by Implen N50 to confirm that all the soil samples were proper for sequencing. The universal primer sets 338 F (5'-ACTCCTACGGGAGGCAGCA-3')/806 R (5'-GGACTACHVGGGTWTCTAAT-3'), and ITS1F (5'-CTTGGTCATTTAGAGGAAGTAA-3')/ITS2 (5'-GCTGCGTTCTTCATCGATGC-3) were used to amplify the V3-V4 variable regions of bacterial 16 S rRNA genes, and fungal internal transcribed spaced (ITS) genes, respectively[80,81]. Polymerase chain reaction (PCR) amplification was performed in 2720 Thermal Cycler (Applied Biosystems) with a 50 μL reaction mixture containing 1 μL of template DNA, 2 μL of forward and reverse primer (10 μM), 25 μL of Taq PCR Master Mix (B630293, BBI Life Sciences Corp.), and 20 μL of ddH_2O under the following cycling procedure: pre-denaturation at 95 °C for 3 min, 35 cycles of denaturation at 95 °C for 30 s, annealing at 57 °C for 30 s, and extension at 72 °C for 30 s; post extension at 72 °C for 8 min[79].

After purification, the PCR products were ready for downstream sequencing. Next-generation sequencing (NGS) was conducted by Allwegene Tech (Beijing, China) using the Illumina HiSeq 2500 platform (Illumina, CA, USA). The raw paired-end sequences were submitted to NCBI GenBank.

Afterward, the Illumina NGS sequences of bacteria and fungi were processed and analyzed using the Quantitative Insights into Microbial Ecology 2 pipeline (QIIME 2, https://qiime2.org/) and PIPITS (https://github.com/hsgweon/pipits), respectively. The taxonomic analysis of bacteria was conducted against the Greengene 13.8 database, while the analysis of fungi was performed using the UNITE Fungal ITS reference database. Due to limitations in current reference databases and the inherent complexity of these samples, a large portion of the fungal communities remained unidentified. Additionally, the α-diversity indices of soil bacterial and fungal communities, including observed OTUs, Shannon–Wiener Index, Simpson Index, and Pielou's Evenness Index, were calculated by QIIME2.

Statistical analyses. Mean ± standard deviation (S.D.) was used to report OCS fluxes and soil biogeochemical properties. The statistical significance of differences in means between different sites or treatments was determined by analysis of variance (ANOVA) and Least Significant Difference test (LSD) at $p = 0.05$ level. The correlations between OCS fluxes and environmental factors were assessed by Pearson correlation analysis.

Principal coordinates analysis (PCoA) and canonical correspondence analysis (CCA) were conducted with CANOCO 5.0 (Microcomputer Power, Ithaca, NY, USA) to explore the differences in microbial community structures and their relationships with soil physicochemical properties. For the network analysis, a Spearman correlation matrix was generated using the R programming language and psych 2.1.9 package, and plotted by Gephi 0.9.7 to further describe the relationships between soil physicochemical properties and microbial communities at the genus level individually (only including genera present in at least five of the twelve samples).

Data availability

All data that support the findings of this study is presented in the manuscript and its supporting information. Figure source data are available on Zenodo repository with a DOI number: 10.5281/zenodo.8116208.

Received: 15 March 2023; Accepted: 5 September 2023;
Published online: 16 September 2023

References

1. Brühl, C., Lelieveld, J., Crutzen, P. J. & Tost, H. The role of carbonyl sulphide as a source of stratospheric sulphate aerosol and its impact on climate. *Atmos. Chem. Phys.* **12**, 1239–1253 (2012).
2. Zumkehr, A. et al. Global gridded anthropogenic emissions inventory of carbonyl sulfide. *Atmos. Environ.* **183**, 11–19 (2018).
3. Lennartz, S. T., Gauss, M., von Hobe, M. & Marandino, C. A. Monthly resolved modelled oceanic emissions of carbonyl sulphide and carbon disulphide for the period 2000–2019. *Earth Syst. Sci. Data* **13**, 2095–2110 (2021).
4. Stinecipher, J. R. et al. Biomass burning unlikely to account for missing source of carbonyl sulfide. *Geophys. Res. Lett.* **46**, 14912–14920 (2019).
5. Belviso, S., Nguyen, B. C. & Allard, P. Estimate of carbonyl sulfide (OCS) volcanic source strength deduced from OCS/CO_2 ratios in volcanic gases. *Geophys. Res. Lett.* **13**, 133–136 (1986).
6. Whelan, M. E., Min, D.-H. & Rhew, R. C. Salt marsh vegetation as a carbonyl sulfide (COS) source to the atmosphere. *Atmos. Environ.* **73**, 131–137 (2013).
7. Saheb, V., Alizadeh, M., Rezaei, F. & Shahidi, S. Quantum chemical and theoretical kinetics studies on the reaction of carbonyl sulfide with H, OH and O(3P). *Computat. Theor. Chem.* **994**, 25–33 (2012).
8. Lin, Y., Sim, M. S. & Ono, S. Multiple-sulfur isotope effects during photolysis of carbonyl sulfide. *Atmos. Chem. Phys.* **11**, 10283–10292 (2011).
9. Protoschill-Krebs, G., Wilhelm, C. & Kesselmeier, J. Consumption of carbonyl sulphide (COS) by higher plant carbonic anhydrase (CA). *Atmos. Environ.* **30**, 3151–3156 (1996).
10. Liu, J. et al. Exchange of carbonyl sulfide (COS) between the atmosphere and various soils in China. *Biogeosciences* **7**, 753–762 (2010).
11. Abadie, C. et al. Global modelling of soil carbonyl sulfide exchanges. *Biogeosciences* **19**, 2427–2463 (2022).
12. Montzka, S. A. et al. On the global distribution, seasonality, and budget of atmospheric carbonyl sulfide (COS) and some similarities to CO_2. *J. Geophys. Res. Atmos.* **112**, D09302 (2007).
13. Geng, C. & Mu, Y. Carbonyl sulfide and dimethyl sulfide exchange between trees and the atmosphere. *Atmos. Environ.* **40**, 1373–1383 (2006).
14. Berry, J. et al. A coupled model of the global cycles of carbonyl sulfide and CO_2: a possible new window on the carbon cycle. *J. Geophys. Res. Biogeosci.* **118**, 842–852 (2013).
15. Maignan, F. et al. Carbonyl sulfide: comparing a mechanistic representation of the vegetation uptake in a land surface model and the leaf relative uptake approach. *Biogeosciences* **18**, 2917–2955 (2021).
16. Kooijmans, L. M. J. et al. Evaluation of carbonyl sulfide biosphere exchange in the Simple Biosphere Model (SiB4). *Biogeosciences* **18**, 6547–6565 (2021).
17. Whelan, M. E. et al. Reviews and syntheses: Carbonyl sulfide as a multi-scale tracer for carbon and water cycles. *Biogeosciences* **15**, 3625–3657 (2018).
18. Gimeno, T. E. et al. Bryophyte gas-exchange dynamics along varying hydration status reveal a significant carbonyl sulphide (COS) sink in the dark and COS source in the light. *New Phytologist* **215**, 965–976 (2017).
19. Asaf, D. et al. Ecosystem photosynthesis inferred from measurements of carbonyl sulphide flux. *Nat. Geosci.* **6**, 186–190 (2013).
20. Hu, L. et al. COS-derived GPP relationships with temperature and light help explain high-latitude atmospheric CO_2 seasonal cycle amplification. *Proc. Natl. Acad. Sci.* **118**, e2103423118 (2021).
21. Whelan, M. E. et al. Soil carbonyl sulfide (OCS) fluxes in terrestrial ecosystems: an empirical model. *J. Geophys. Res. Biogeosci.* **127**, e2022JG006858 (2022).
22. Whelan, M. E. & Rhew, R. C. Carbonyl sulfide produced by abiotic thermal and photodegradation of soil organic matter from wheat field substrate. *J. Geophys. Res. Biogeosci.* **120**, 54–62 (2015).
23. Kato, H., Saito, M., Nagahata, Y. & Katayama, Y. Degradation of ambient carbonyl sulfide by Mycobacterium spp. in soil. *Microbiology* **154**, 249–255 (2008).
24. Ogawa, T., Kato, H., Higashide, M., Nishimiya, M. & Katayama, Y. Degradation of carbonyl sulfide by Actinomycetes and detection of clade D of β-class carbonic anhydrase. *FEMS Microbiol. Lett.* **363**, fnw223 (2016).
25. Kitz, F. et al. Soil carbonyl sulfide exchange in relation to microbial community composition: insights from a managed grassland soil amendment experiment. *Soil Biol. Biochem.* **135**, 28–37 (2019).
26. Meredith, L. K. et al. Soil exchange rates of COS and $CO^{18}O$ differ with the diversity of microbial communities and their carbonic anhydrase enzymes. *ISME J.* **13**, 290–300 (2019).
27. Li, W., Yu, L., Yuan, D., Wu, Y. & Zeng, X. A study of the activity and ecological significance of carbonic anhydrase from soil and its microbes from different karst ecosystems of Southwest China. *Plant Soil* **272**, 133–141 (2005).
28. Sharma, A., Bhattacharya, A. & Singh, S. Purification and characterization of an extracellular carbonic anhydrase from Pseudomonas fragi. *Process Biochem.* **44**, 1293–1297 (2009).
29. Seefeldt, L. C., Rasche, M. E. & Ensign, S. A. Carbonyl sulfide and carbon dioxide as new substrates, and carbon disulfide as a new inhibitor, of nitrogenase. *Biochemistry* **34**, 5382–5389 (1995).
30. Bunk, R., Behrendt, T., Yi, Z., Andreae, M. O. & Kesselmeier, J. Exchange of carbonyl sulfide (OCS) between soils and atmosphere under various CO_2 concentrations. *J. Geophys. Res. Biogeosci.* **122**, 1343–1358 (2017).
31. Meredith, L. K. et al. Coupled biological and abiotic mechanisms driving carbonyl sulfide production in soils. *Soil Syst.* **2**, 37 (2018).
32. Katayama, Y., Kanagawa, T. & Kuraishi, H. Emission of carbonyl sulfide by Thiobacillus thioparus grown with thiocyanate in pure and mixed cultures. *FEMS Microbiol. Lett.* **114**, 223–227 (1993).
33. Smeulders, M. J. et al. Bacterial CS_2 hydrolases from acidithiobacillus thiooxidans strains are homologous to the archaeal catenane CS_2 hydrolase. *J. Bacteriol.* **195**, 4046–4056 (2013).
34. Maseyk, K. et al. Sources and sinks of carbonyl sulfide in an agricultural field in the Southern Great Plains. *PNAS* **111**, 9064–9069 (2014).

35. Wang, J., Wang, Y., Wang, X. & Sun, L. Penguins and vegetations on Ardley Island, Antarctica: evolution in the past 2400 years. *Polar Biol.* **30**, 1475–1481 (2007).
36. Terauds, A. & Lee, J. R. Antarctic biogeography revisited: updating the Antarctic conservation biogeographic regions. *Divers. Distrib.* **22**, 836–840 (2016).
37. Chen, Y., Shen, L., Huang, T., Chu, Z. & Xie, Z. Transformation of sulfur species in lake sediments at Ardley Island and Fildes Peninsula, King George Island, Antarctic Peninsula. *Sci. Total Environ.* **703**, 135591 (2020).
38. Lee, J. R. et al. Climate change drives expansion of Antarctic ice-free habitat. *Nature* **547**, 49–54 (2017).
39. IPCC. Climate Change 2021: The Physical Science Basis. Contribution of Working Group I to the Sixth Assessment Report of the Intergovernmental Panel on Climate Change [Masson-Delmotte, V., et al (eds.)]. (Cambridge University Press, 2021).
40. Sun, L., Xie, Z. & Zhao, J. A 3,000-year record of penguin populations. *Nature* **407**, 858 (2000).
41. Sun, L. et al. A 1,500-year record of Antarctic seal populations in response to climate change. *Polar Biol.* **27**, 495–501 (2004).
42. Yi, Z., Wang, X., Sheng, G. & Fu, J. Exchange of carbonyl sulfide (OCS) and dimethyl sulfide (DMS) between rice paddy fields and the atmosphere in subtropical China. *Agriculture, Ecosyst. Environ.* **123**, 116–124 (2008).
43. Yi, Z. & Wang, X. Carbonyl sulfide and dimethyl sulfide fluxes in an urban lawn and adjacent bare soil in Guangzhou, China. *J. Environ. Sci.* **23**, 784–789 (2011).
44. Whelan, M. E. & Rhew, R. C. Reduced sulfur trace gas exchange between a seasonally dry grassland and the atmosphere. *Biogeochemistry* **128**, 267–280 (2016).
45. Kitz, F. et al. In situ soil COS exchange of a temperate mountain grassland under simulated drought. *Oecologia* **183**, 851–860 (2017).
46. Kesselmeier, J., Teusch, N. & Kuhn, U. Controlling variables for the uptake of atmospheric carbonyl sulfide by soil. *J. Geophys. Res. Atmos.* **104**, 11577–11584 (1999).
47. Bhattacharya, A., Shrivastava, A. & Sharma, A. Evaluation of enhanced thermostability and operational stability of carbonic anhydrase from micrococcus species. *Appl. Biochem. Biotechnol.* **170**, 756–773 (2013).
48. Nathan, V. K. & Ammini, P. Carbon dioxide sequestering ability of bacterial carbonic anhydrase in a mangrove soil microcosm and its bio-mineralization properties. *Water Air Soil Pollut* **230**, 192 (2019).
49. Shen, L., Huang, T., Chen, Y., Chu, Z. & Xie, Z. Diverse transformations of sulfur in seabird-affected sediments revealed by microbial and stable isotope analyses. *J. Ocean. Limnol.* 1–12 https://doi.org/10.1007/s00343-021-1173-z (2022).
50. Xie, Z.-Q., Sun, L.-G., Wang, J.-J. & Liu, B.-Z. A potential source of atmospheric sulfur from penguin colony emissions. *J. Geophys. Res. Atmos.* **107**, ACH 5-1–ACH 5-10 (2002).
51. Chavez, C. et al. The impact of supplemental dietary methionine sources on volatile compound concentrations in broiler excreta. *Poultry Sci.* **83**, 901–910 (2004).
52. Trabue, S. et al. Field sampling method for quantifying volatile sulfur compounds from animal feeding operations. *Atmos. Environ.* **42**, 3332–3341 (2008).
53. Kaisermann, A. et al. Disentangling the rates of carbonyl sulfide (COS) production and consumption and their dependency on soil properties across biomes and land use types. *Atmos. Chem. Phys.* **18**, 9425–9440 (2018).
54. Kanda, K., Tsuruta, H. & Minami, K. Emission of dimethyl sulfide, carbonyl sulfide, and carbon bisulfide from paddy fields. *Soil Sci. Plant Nutr.* **38**, 709–716 (1992).
55. Yang, Z., Kanda, K., Tsuruta, H. & Minami, K. Measurement of biogenic sulfur gases emission from some Chinese and Japanese soils. *Atmos. Environ.* **30**, 2399–2405 (1996).
56. Wolf, D. C., Dao, T. H., Scott, H. D. & Lavy, T. L. Influence of sterilization methods on selected soil microbiological, physical, and chemical properties. *J. Environ. Quality* **18**, 39–44 (1989).
57. Gries, C., Nash, T. H. & Kesselmeier, J. Exchange of reduced sulfur gases between lichens and the atmosphere. *Biogeochemistry* **26**, 25–39 (1994).
58. Kuhn, U. et al. Carbonyl sulfide exchange on an ecosystem scale: soil represents a dominant sink for atmospheric COS. *Atmos. Environ.* **33**, 995–1008 (1999).
59. Kuhn, U. & Kesselmeier, J. Environmental variables controlling the uptake of carbonyl sulfide by lichens. *J. Geophys. Res. Atmos.* **105**, 26783–26792 (2000).
60. Rastogi, B. et al. Ecosystem fluxes of carbonyl sulfide in an old-growth forest: temporal dynamics and responses to diffuse radiation and heat waves. *Biogeosciences* **15**, 7127–7139 (2018).
61. Rastogi, B. et al. Large uptake of atmospheric OCS observed at a moist old growth forest: controls and implications for carbon cycle applications. *J. Geophys. Res. Biogeosci.* **123**, 3424–3438 (2018).
62. Stimler, K., Montzka, S. A., Berry, J. A., Rudich, Y. & Yakir, D. Relationships between carbonyl sulfide (COS) and CO_2 during leaf gas exchange. *New Phytologist* **186**, 869–878 (2010).
63. Aro, E.-M. & Gerbaud, A. Photosynthesis and Photorespiration in Mosses. in *Advances in Photosynthesis Research: Proceedings of the VIth International Congress on Photosynthesis, Brussels, Belgium, August 1–6, 1983 Volume 3* (ed. Sybesma, C.) 867–870 (Springer Netherlands, 1984). https://doi.org/10.1007/978-94-017-4973-2_198.
64. Kubásek, J., Hájek, T., Duckett, J., Pressel, S. & Šantrůček, J. Moss stomata do not respond to light and CO_2 concentration but facilitate carbon uptake by sporophytes: a gas exchange, stomatal aperture, and ^{13}C-labelling study. *New Phytologist* **230**, 1815–1828 (2021).
65. Gerdel, K., Spielmann, F. M., Hammerle, A. & Wohlfahrt, G. Eddy covariance carbonyl sulfide flux measurements with a quantum cascade laser absorption spectrometer. *Atmos. Meas. Tech.* **10**, 3525–3537 (2017).
66. Berkelhammer, M. et al. Constraining surface carbon fluxes using in situ measurements of carbonyl sulfide and carbon dioxide. *Global Biogeochem. Cycles* **28**, 161–179 (2014).
67. Commane, R. et al. Seasonal fluxes of carbonyl sulfide in a midlatitude forest. *PNAS* **112**, 14162–14167 (2015).
68. Kooijmans, L. M. J. et al. Canopy uptake dominates nighttime carbonyl sulfide fluxes in a boreal forest. *Atmos. Chem. Phys.* **17**, 11453–11465 (2017).
69. Wehr, R. et al. Dynamics of canopy stomatal conductance, transpiration, and evaporation in a temperate deciduous forest, validated by carbonyl sulfide uptake. *Biogeosciences* **14**, 389–401 (2017).
70. Zhang, W. et al. Chloroform ($CHCl_3$) emissions from Coastal Antarctic Tundra. *Geophys. Res. Lett.* **48**, e2021GL093811 (2021).
71. Ogée, J. et al. A new mechanistic framework to predict OCS fluxes from soils. *Biogeosciences* **13**, 2221–2240 (2016).
72. Whelan, M. E. et al. Carbonyl sulfide exchange in soils for better estimates of ecosystem carbon uptake. *Atmos. Chem. Phys.* **16**, 3711–3726 (2016).
73. Zhu, R. et al. Tropospheric phosphine and its sources in coastal Antarctica. *Environ. Sci. Technol.* **40**, 7656–7661 (2006).
74. Zhu, R. et al. Nitrous oxide emissions from sea animal colonies in the maritime Antarctic. *Geophys. Res. Lett.* **35**, L09807 (2008).
75. Zhang, W. et al. Atmospheric CCl_4 degradation in Antarctic tundra soils and the evaluation on its partial atmospheric lifetime with respect to soil. *Sci. Total Environ.* **835**, 155449 (2022).
76. Khan, M. A. H., Whelan, M. E. & Rhew, R. C. Effects of temperature and soil moisture on methyl halide and chloroform fluxes from drained peatland pasture soils. *J. Environ. Monit.* **14**, 241–249 (2012).
77. de Mello, W. Z. & Hines, M. E. Application of static and dynamic enclosures for determining dimethyl sulfide and carbonyl sulfide exchange in Sphagnum peatlands: implications for the magnitude and direction of flux. *J. Geophys. Res. Atmos.* **99**, 14601–14607 (1994).
78. Suárez, I., Salmerón-García, A., Cabeza, J., Capitán-Vallvey, L. F. & Navas, N. Development and use of specific ELISA methods for quantifying the biological activity of bevacizumab, cetuximab and trastuzumab in stability studies. *J. Chromatogr. B* **1032**, 155–164 (2016).
79. Jiang, S. et al. Airborne microbial community structure and potential pathogen identification across the PM size fractions and seasons in the urban atmosphere. *Sci. Total Environ.* **831**, 154665 (2022).
80. Orgiazzi, A. et al. Unravelling soil fungal communities from different mediterranean land-use backgrounds. *PLoS ONE* **7**, e34847 (2012).
81. Lee, C. K., Barbier, B. A., Bottos, E. M., McDonald, I. R. & Cary, S. C. The inter-valley soil comparative survey: the ecology of dry valley edaphic microbial communities. *ISME J* **6**, 1046–1057 (2012).

Acknowledgements

This study was jointly funded by the National Natural Science Foundation of China (No. 41976220), National Key Research and Development Program of China (No. 2020YFA0608501), China Postdoctoral Science Foundation (No. 2022M713042), and Fundamental Research Funds for Central Universities (No. WK2080000170). RR would like to thank the Danish National Research Foundation for supporting the activities within the Center for Volatile Interactions (No. DNRF168). The authors would like to thank Professor Zhigang Yi for assistance in GC/MS analysis, the Chinese National Antarctic Research Expedition (CHINARE) for assistance in fieldwork.

Author contributions

R.Z. and W.Z. conceived and secured funding for the study. W.Z. and Y.J. conducted the main laboratory experiments with assistance from R.C.R. Fieldwork was carried out by B.S. Soil property measurements and microbial and enzyme analysis was performed by W.Z. and B.S. Data analysis was conducted by W.Z., Y.J., B.S., and Z.Z. The manuscript was prepared by W.Z. with contributions from all authors, particularly R.Z. and R.R.

Competing interests

The authors declare no competing interests.

Additional information

Supplementary information The online version contains supplementary material available at https://doi.org/10.1038/s43247-023-00990-4.

Correspondence and requests for materials should be addressed to Renbin Zhu.

Peer review information *Communications Earth & Environment* thanks Kadmiel Maseyk, Nathan Vinod Kumar and the other, anonymous, reviewer(s) for their contribution to the peer review of this work. Primary Handling Editors: Kate Buckeridge and Clare Davis. A peer review file is available.